The Plant Cell, Vol. 32: 1919–1932, June 2020, www.plantcell.org © 2020 ASPB.

Control of Plant Branching by the CUC2/CUC3-DA1-UBP15 Regulatory Module

Yu Li,[a,b,1] Tian Xia,[a,b,1] Fan Gao,[a,b] and Yunhai Li[a,b,2]

[a] State Key Laboratory of Plant Cell and Chromosome Engineering, Chinese Academy of Sciences Centre for Excellence in Molecular Plant Science, Institute of Genetics and Developmental Biology, The Innovative Academy of Seed Design, Chinese Academy of Sciences, Beijing 100101, People's Republic of China
[b] University of Chinese Academy of Sciences, Beijing 100039, China

ORCID IDs: 0000-0002-0545-6475 (Yu.L.); 0000-0002-0053-9263 (T.X.); 0000-0002-8668-6781 (F.G.); 0000-0002-0025-4444 (Y.L.)

Lateral branches are important for plant architecture and production, but how plants determine their lateral branches remains to be further understood. Here, we report that the CUP-SHAPED COTYLEDON2 (CUC2)/CUC3-DA1-UBIQUITIN-SPECIFIC PROTEASE15 (UBP15) regulatory module controls the initiation of axillary meristems, thereby determining the number of lateral branches in Arabidopsis (*Arabidopsis thaliana*). Mutation in the ubiquitin-dependent peptidase DA1 causes fewer lateral branches due to defects in the initiation of axillary meristems. The transcription factors CUC2 and CUC3, which regulate the axillary meristem initiation, directly bind to the *DA1* promoter and activate its expression. Further results show that UBP15, which is a direct substrate of DA1 peptidase, represses the initiation of axillary meristems. Genetic analyses support that CUC2/CUC3, DA1, and UBP15 function, at least in part, in a common pathway to regulate the initiation of axillary meristems. Therefore, our findings establish a genetic and molecular framework by which the CUC2/CUC3-DA1-UBP15 regulatory module controls the initiation of axillary meristems, thereby determining plant architecture.

INTRODUCTION

The diversity of forms in flowering plants is mainly decided by the number, position, and shape of lateral organs in the aerial part of plants; these lateral organs arise from the shoot apical meristem (SAM) and other secondary meristems (Pautler et al., 2013). Branches are important lateral organs that affect plant architecture and plant yield (Wang and Li, 2008; Wang et al., 2018). A branch originates from a secondary meristem in the axil of leaves, referred to as the axillary meristem (AM; Grbic and Bleecker, 2000). The AM can develop into an axillary bud and then form a branch (Schmitz and Theres, 2005; Domagalska and Leyser, 2011). In some conditions, the AMs develop into axillary buds but remain dormant (Napoli et al., 1999). The axillary bud can later develop into a complete branch, depending on environmental and developmental cues. Therefore, the development of branches can be divided into two main steps: the initiation of AMs and the outgrowth of axillary buds (Tantikanjana et al., 2001). Strigolactones act as a major player in regulating bud outgrowth (Domagalska and Leyser, 2011; Waters et al., 2012; Brewer et al., 2013; Smith and Li, 2014; Flematti et al., 2016). Auxins and strigolactones negatively regulate the outgrowth of axillary buds (McSteen and Leyser, 2005; Brewer et al., 2015), and cytokinins function antagonistically with auxins and strigolactones to promote the outgrowth of axillary buds (Müller and Leyser, 2011; Janssen et al., 2014; Barbier et al., 2019).

Several transcription factors influence the initiation of AMs, thereby influencing the formation of plant branches. *LATERAL SUPPRESSOR* (*LS*) in tomato (*Solanum lycopersicum*), *LATERAL SUPPRESSOR* in Arabidopsis (*Arabidopsis thaliana*; *LAS*), and *MONOCULM1* (*MOC1*) in rice (*Oryza sativa*), which encode the GRAS transcription factors (Greb et al., 2003), regulate AM initiation. The tomato *BLIND* gene, which encodes an MYB transcription factor, promotes the AM initiation (Schmitz et al., 2002). Its Arabidopsis homologs REGULATORS OF AXILLARY MERISTEMS act redundantly to promote the establishment of AMs during both vegetative and reproductive growth phases (Keller et al., 2006; Müller et al., 2006). NAC transcriptional factors CUP-SHAPED COTYLEDON (CUC) regulate the AM initiation in leaf axils of rosette leaves in Arabidopsis (Hibara et al., 2006; Raman et al., 2008). In addition, MYB transcription factors LATERAL ORGAN FUSION1 (LOF1) and LOF2 and classIII homeodomain/leucine zipper transcription factor REVOLUTA affect multiple growth and developmental processes including the AM initiation (Otsuga et al., 2001; Lee et al., 2009). Recent studies further uncovered the gene regulatory network in the AM initiation through genome-scale analyses (Tian et al., 2014). CUC2 and LAS work as two hubs of this gene regulatory network. CUC2 proteins directly bind to the promoter of *LAS* and activate its expression (Hibara et al., 2006; Raman et al., 2008; Tian et al., 2014). An auxin minimum has been proposed to be required for the AM initiation (Wang et al., 2014a, 2014b). Cytokinin biosynthesis and signaling also affect normal AM initiation (Wang et al., 2014b; Müller et al., 2015). Therefore, these studies show that multiple factors and signaling pathways influence the initiation of AMs.

We have previously reported that DA1, a ubiquitin-dependent peptidase, regulates seed and organ size in Arabidopsis (Li et al., 2008; Xia et al., 2013; Du et al., 2014; Dong et al., 2017). Here, we uncover a function for DA1 in the regulation of the AM initiation.

[1] These authors contributed equally to this work.
[2] Address correspondence to yhli@genetics.ac.cn.
The author responsible for distribution of materials integral to the findings presented in this article in accordance with the policy described in the Instructions for Authors (www.plantcell.org) is: Yunhai Li (yhli@genetics.ac.cn).
www.plantcell.org/cgi/doi/10.1105/tpc.20.00012

IN A NUTSHELL

Background: The diversity of higher plant forms is determined by the number, position, and shape of lateral organs in the aerial parts of plants. Branches are important lateral organs, which affect plant architecture and plant yield. Branches originate from secondary meristems in the axils of leaves, referred to as the axillary meristems. The axillary meristems can develop into axillary buds and then form branches. However, in some conditions, the axillary meristems develop into axillary buds and stay in dormancy. The axillary bud can also develop into a complete branch depending on environmental and developmental cues. Therefore, the development of a branch can be divided into two main steps: the initiation of axillary meristems and the outgrowth of axillary buds.

Question: Several genes affect axillary meristem initiation in Arabidopsis, but the mechanisms of axillary meristem initiation are still largely unknown. Here, we uncover a new regulatory module CUC2/CUC3-DA1-UBP15 that controls the initiation of axillary meristems, thereby determining plant architecture.

Findings: Mutation in the ubiquitin-dependent peptidase DA1 causes fewer lateral branches due to defects in the initiation of axillary meristems. The transcription factors CUC2 and CUC3, which regulate the initiation of the axillary meristems, directly bind to the promoter of *DA1* and activate its expression. Further results show that the ubiquitin specific protease UBP15, which is a direct substrate of DA1 peptidase, represses the initiation of axillary meristems. Genetic analyses support that *CUC2*/*CUC3*, *DA1* and *UBP15* function in a common pathway to control the initiation of axillary meristems. Therefore, our findings reveal a genetic and molecular framework in which the CUC2/CUC3-DA1-UBP15 regulatory module controls the initiation of axillary meristems, thereby determining plant architecture.

Next steps: It is important to investigate which environmental cues and endogenous signals regulate the CUC2/CUC3-DA1-UBP15 pathway. It is also essential to identify the targets of UBP15 in the axillary meristem initiation. Considering that DA1 and UBP15 and their homologs in crops influence seed yield, it will be worthwhile to investigate whether homologs of CUC2/CUC3, DA1 and UBP15 in crops could be used to improve plant architecture in key crops.

The *da1-1* single mutant forms fewer lateral branches due to defects in the initiation of AMs. The transcription factors CUC2 and CUC3 associate with the promoter of *DA1* and activate the expression of *DA1*. The mutation in the ubiquitin-specific protease UBP15, which is a direct substrate of DA1 peptidase, promotes the AM initiation. Genetic analyses demonstrate that CUC2/CUC3, DA1, and UBP15 function, at least in part, in a common pathway to regulate the initiation of AMs. Therefore, our findings reveal that the CUC2/CUC3-DA1-UBP15 regulatory module controls the initiation of AMs, thereby influencing plant architecture in Arabidopsis.

RESULTS

The *da1-1* Mutant Produces Fewer Branches

We have previously shown that DA1 regulates seed and organ size by influencing cell proliferation in Arabidopsis (Li et al., 2008). The *da1-1* mutant also produced fewer branches compared with the wild type (Columbia [Col-0]) in long-day conditions (Supplemental Figure 1A). We therefore investigated the development of axillary buds in 45-d-old Col-0 and *da1-1* rosette leaf axils in long-day conditions (Supplemental Figure 1B). In most Col-0 plants, the axils of the first pair of rosette leaves contained axillary buds. By contrast, in most *da1-1* plants, we did not observe axillary buds in the leaf axils of the first pair of rosette leaves. In addition, the development of axillary buds was delayed in *da1-1* (Supplemental Figure 1B).

When plants were first grown in short-day conditions for 28 d and then moved to long-day conditions, the axillary branches in *da1-1* were strongly reduced compared with those in the wild type (Figure 1A). Most wild-type plants contained axillary buds in the axils of the third to late rosette leaves, although a majority of the wild-type plants had no axillary buds in the axils of the first pair of leaves (Figure 1D). By contrast, most *da1-1* plants had no axillary buds in the axils of the first to sixth rosette leaves (Figure 1D). We frequently observed that *da1-1* lacked axillary buds in the axils of late rosette leaves (Figures 1B and 1D). Axillary buds were also absent from a few cauline leaf axils in *da1-1* (Figures 1C and 1D). These results indicate that DA1 regulates the formation of axillary branches.

The *da1-1* allele encodes a mutant protein DA1^{R358K}, which negatively affects the function of DA1 and its closest homolog DAR1, although *da1-1*/+ heterozygous plants do not show obvious alterations in seed- and organ-size phenotypes (Li et al., 2008). Double *da1-knockout1* (*da1-ko1*) *dar1-1* T-DNA insertion mutants exhibit large seeds and organs, like those observed in the *da1-1* mutant, while *da1-ko1* and *dar1-1* single mutants do not show an obvious large seed phenotype (Li et al., 2008). We examined whether *da1-ko1*, *dar1-1*, and *da1-ko1 dar1-1* double mutations affected the formation of axillary branches. The *da1-ko1 dar1-1* double mutant also exhibited fewer lateral branches compared to the wild type (Figures 1A and 1D). Axillary buds were absent from a few rosette and cauline leaf axils in *da1-ko1 dar1-1* (Figures 1B and 1C). The *da1-ko1* and *dar1-1* single mutants did not show an obvious branch-defect phenotype (Supplemental Figures 1C to 1E). As overexpression of the DA1^{R358K} protein (*35S*:*DA1$^{R/K}$*) in the wild type has a dominant-negative effect on organ growth (Li et al., 2008), we investigated whether *35S*:*DA1$^{R/K}$* plants had the defects in the formation of axillary buds. Compared with the wild-type plants, *35S*:*DA1$^{R/K}$* plants exhibited fewer branches and axillary buds (Figures 1A to 1D; Supplemental Figure 2). By contrast, overexpression of *DA1* (*35S*:*DA1*) very slightly increased the branch number compared with the Col-0 plants (Supplemental Figure 3). A genomic fragment of *DA1* (*DA1COM*) complemented

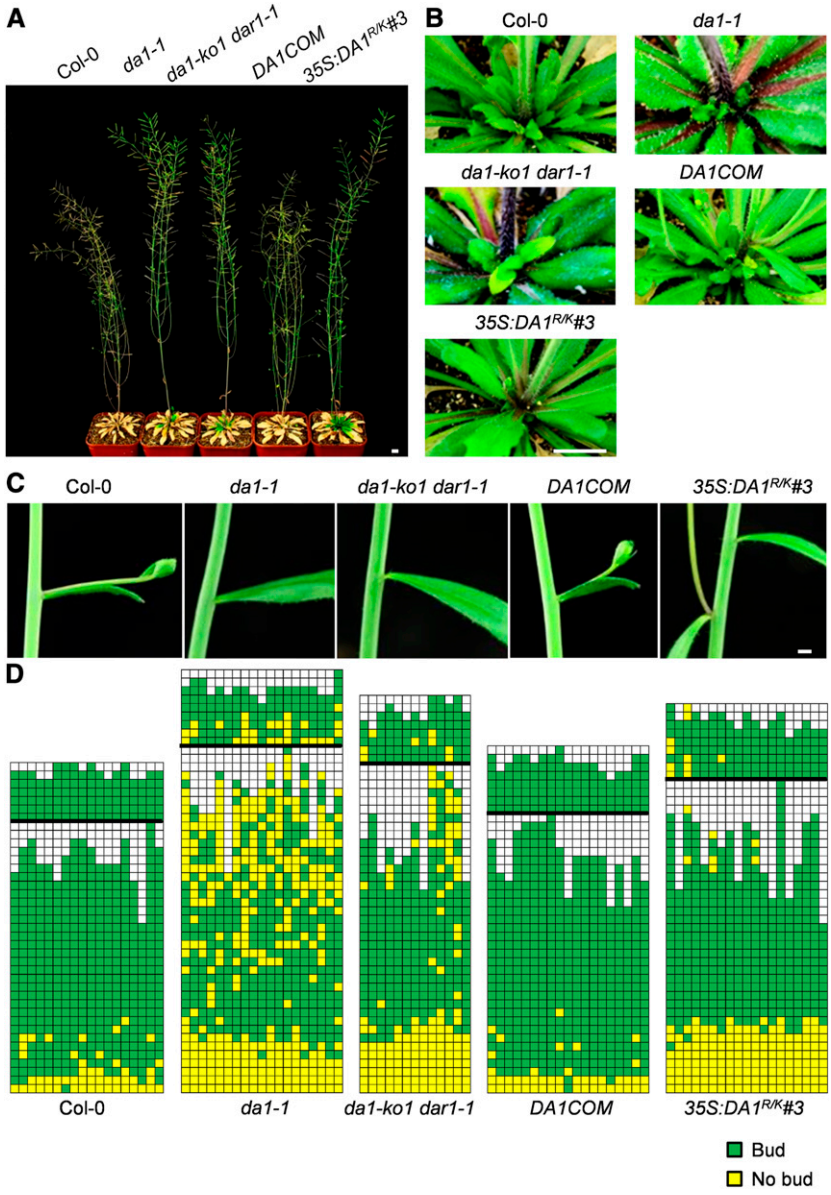

Figure 1. *da1-1* Mutant Produces Fewer Branches.

(A) Plants of Col-0, *da1-1*, *da1-ko1 dar1-1*, *DA1COM*, and *35S:DA1*$^{R/K}$*#3*. The *da1-1* mutant produces fewer branches than the wild type (Col-0). Plants were grown for 28 d in short photoperiods and subsequently grown for 60 d under long-day conditions.

(B) Close-up views of rosette leaf branches in Col-0, *da1-1*, *da1-ko1 dar1-1*, *DA1COM*, and *35S:DA1*$^{R/K}$*#3* plants. The *da1-1*, *da1-ko1 dar1-1*, and *35S:DA1*$^{R/K}$ produce fewer branches than Col-0.

(C) Close-up views of cauline leaf branches in Col-0, *da1-1*, *da1-ko1 dar1-1*, *DA1COM*, and *35S:DA1*$^{R/K}$*#3* plants. Cauline leaves of Col-0 form branches in their axils, while *da1-1*, *da1-ko1 dar1-1*, and *35S:DA1*$^{R/K}$#3 frequently failed to produce branches.

(D) Schematic representation of axillary branch or bud formation in individual leaf axils of Col-0, *da1-1*, *da1-ko1 dar1-1*, *DA1COM*, and *35S:DA1*$^{R/K}$*#3* plants. The thick black horizontal line represents the border between the youngest rosette leaf and the oldest cauline leaf, with positions of progressively younger cauline leaves above the line, and positions of progressively older rosette leaves below it. Each column represents a single plant, and each square within a column represents an individual leaf axil shown from youngest (top) to oldest. Green indicates the presence of an axillary bud, and yellow indicates the absence of an axillary bud in any particular leaf axil. Plants were grown for 28 days in short photoperiods and subsequently shifted to long days ($n \geq 13$). Bar in **(A)** and **(B)** = 1 cm; bar in **(C)** = 1 mm.

the reduced axillary bud phenotype of *da1-1* (Figures 1A to 1D; Li et al., 2008). These results demonstrate that DA1 and its closest homolog DAR1 regulate the formation of lateral branches.

da1-1 Represses the AM Initiation

AMs are formed in rosette and cauline leaf axils and develop into axillary buds and branches in response to environmental and internal signals. Considering that *da1-1* represses the formation of axillary buds, DA1 could regulate the AM initiation. To test this hypothesis, we examined leaf axils in *da1-1* using scanning electron microscopy. The meristem-like structure was not observed in *da1-1* rosette leaf axils that did not produce axillary buds (Figure 2A). These results demonstrate that DA1 and its closest homolog DAR1 are involved in the regulation of the AM initiation.

The AM is marked by the expression of the *SHOOT MERISTEMLESS* (*STM*) gene (Long and Barton, 2000). Considering that DA1 influences the AM initiation, we asked whether the expression of *STM* could be affected by the *da1-1* mutation. We crossed *da1-1* with the *pSTM*:*GUS* reporter and generated *da1-1*;*pSTM*:*GUS* plants. β-Glucuronidase (GUS) activity in the *pSTM*:*GUS* line was detected in the boundary zone between the SAM and leaf primordia (Figure 2C; Kirch et al., 2003; Lee et al., 2009). By contrast, in *da1-1*;*pSTM*:*GUS* plants, GUS activity was reduced in the center of the leaf axils that failed to produce axillary buds (Figure 2C). These results further demonstrate that DA1 controls the initiation of AMs. We then examined whether DA1 could be expressed in the boundary regions using the *pDA1*:*GUS* transgenic line (Li et al., 2008). GUS activity in the *pDA1*:*GUS* line was detected in the shoot meristem, young leaves, the region between the shoot meristem and leaf primordia, and the axils of cauline leaves (Figure 2B). As the region between leaf primordia and the shoot meristem will later form leaf axils, expression of *DA1* is consistent with its role in the AM initiation.

DA1 Acts, at Least in Part, in a Common Pathway with CUC2/CUC3 to Control the Initiation of AMs

Several genes have been described to regulate AM initiation in Arabidopsis, such as *LAS*, *REGULATORS OF AXILLARY MERISTEM*S (*RAX*s), and *CUC*s (Greb et al., 2003; Hibara et al., 2006; Keller et al., 2006; Müller et al., 2006; Raman et al., 2008). The *las* mutants generate almost no branches during vegetative development (Greb et al., 2003). We obtained the *las-101* mutant and observed that nearly all axils of rosette leaves in *las-101* lacked axillary buds (Figure 3; Supplemental Figure 4B; Hibara et al., 2006). The axils of cauline leaves in *las-101* can form branches normally, and most of these branches were fused with main stems (Figure 3; Supplemental Figure 4C), consistent with a previous study (Hibara et al., 2006). We crossed *las-101* with *da1-1* to generate the *da1-1 las-101* double mutant. All axils of rosette leaves in *da1-1 las-101* failed to form the axillary buds, and most axils of cauline leaves in *da1-1 las-101* lacked axillary buds, although the *las-101* single mutation did not affect the AM initiation in axils of cauline leaves (Figure 3; Supplemental Figures 4A to 4C), suggesting that the *las-101* mutation synergistically enhanced the AM initiation-defect phenotype of *da1-1* in both rosette leaf axils and cauline leaf axils. These data also suggest that *DA1* may act redundantly with *LAS* to control the AM initiation during vegetative and reproductive development.

In Arabidopsis, MYB transcription factors RAX1, RAX2, and RAX3 act redundantly to control the initiation of AMs (Keller et al., 2006; Müller et al., 2006). The *rax1* mutant exhibits a moderate defect in the AM initiation of rosette leaf axils, whereas *rax2* and

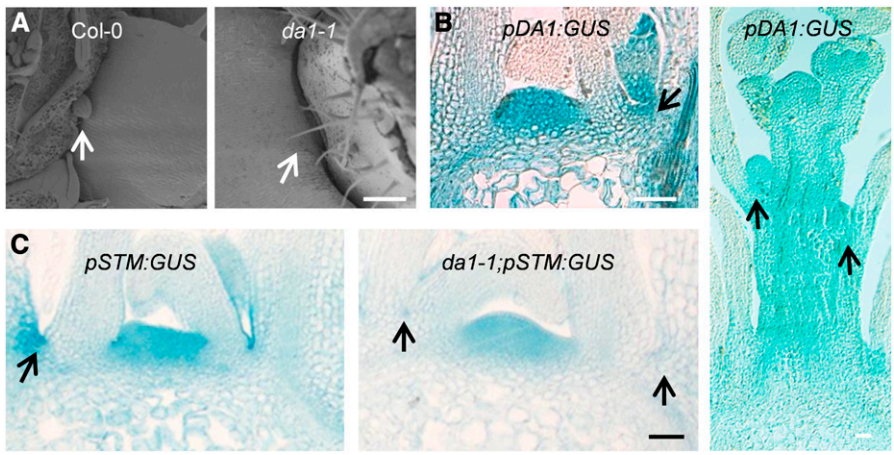

Figure 2. DA1 Regulates the Initiation of Axillary Meristems.

(A) Scanning electron micrographs of a Col-0 rosette leaf axil showing an axillary bud (left, arrow) and a barren *da1-1* rosette leaf axil (right, arrow).
(B) *DA1* expression activity was monitored using *pDA1*:*GUS* transgenic plants. GUS activity is detected in longitudinal section through shoot apex during vegetative development (left, plants grown for 28 d under short-day conditions) and reproductive development (right, plants grown for 28 d under short-day conditions and subsequently shifted to long-day conditions for 6 d).
(C) *pSTM*:*GUS* expression in longitudinal sections of Col-0 and *da1-1*. GUS signal is reduced in leaf axils of *da1-1* plants. Plants were grown for 28 d in short photoperiods.
Bar in **(A)** = 200 μm; bar in **(B)** and **(C)** = 20 μm.

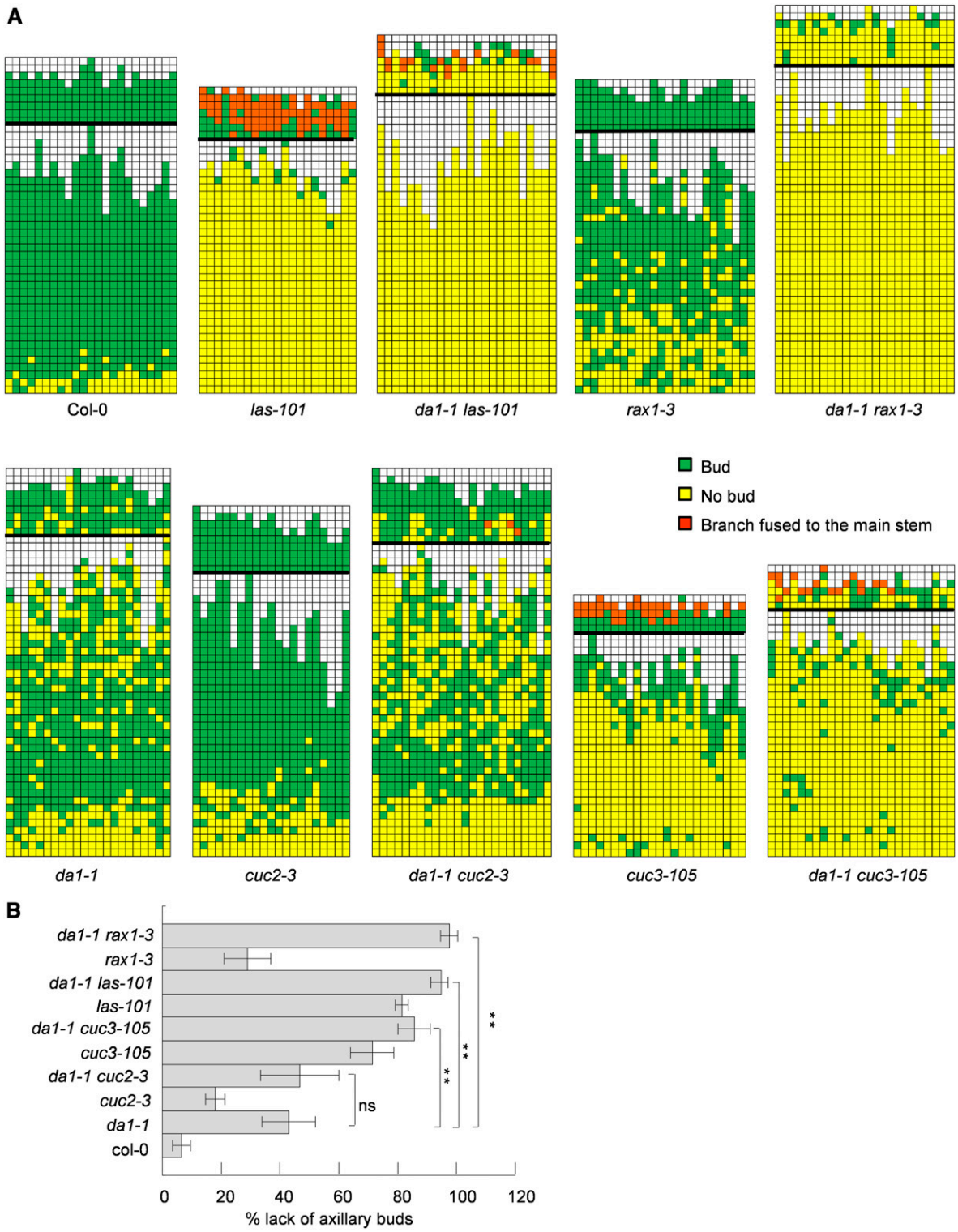

Figure 3. DA1 Acts Genetically with CUC2 and CUC3 to Control the Initiation of Axillary Meristems.

(A) Schematic representation of axillary branch or bud formation in individual leaf axils of Col-0, *da1-1*, *las-101*, *da1-1 las-101*, *rax1-3*, *da1-1 rax1-3*, *cuc2-3*, *da1-1 cuc2-3*, *cuc3-105*, and *da1-1 cuc3-105* plants. The thick black horizontal line represents the border between the youngest rosette leaf and the oldest cauline leaf, with positions of progressively younger cauline leaves above the line and positions of progressively older rosette leaves below the line. Each column represents a single plant, and each square within a column represents an individual leaf axil shown from youngest (top) to oldest. Green indicates the

rax3 single mutants do not show a clear defect (Keller et al., 2006), indicating that RAX1 plays a predominant role in determining the initiation of AMs. We therefore crossed *da1-1* with *rax1-3* to generate the *da1-1 rax1-3* double mutant. Consistent with previous results, the *rax1-3* mutant frequently failed to initiate axillary meristems in the rosette leaf axils (Figure 3; Supplemental Figure 4E), while *rax1-3* showed normal AM initiation in the axils of cauline leaves (Figure 3; Supplemental Figure 4F; Keller et al., 2006). By contrast, the *da1-1 rax1-3* double mutant completely lacked axillary buds in rosette leaf axils, and *da1-1 rax1-3* also failed to initiate AMs in the axils of most cauline leaves (Figure 3; Supplemental Figures 4D to 4F). These genetic analyses reveal a synergistic interaction between *DA1* and *RAX1* in the regulation of the AM initiation during vegetative and reproductive development.

NAC transcription factors CUC1, CUC2, and CUC3 have been reported to participate in diverse plant developmental processes, such as boundary formation and AM initiation during postembryonic development (Aida et al., 1997; Hibara et al., 2006). The *cuc2-3* mutation moderately represses the AM initiation in rosette leaf axils, while *cuc3-105* strongly suppresses the AM initiation in rosette leaf axils and also causes branches to be fused to main stems (Figure 3; Hibara et al., 2006; Raman et al., 2008). By contrast, *cuc1* single mutations do not affect AM initiation (Hibara et al., 2006). To understand genetic interactions of *DA1* with *CUC* genes, we crossed *da1-1* with *cuc2-3* and *cuc3-105* and generated *da1-1 cuc2-3* and *da1-1 cuc3-105* double mutants, respectively. The phenotype of *da1-1 cuc2-3* in the AM initiation was more like that observed in the *da1-1* single mutant during vegetative and reproductive development (Figure 3). The phenotype of the *da1-1 cuc3-105* mutant in AM initiation during vegetative development was more like that observed in the *cuc3-105* single mutant, although the *da1-1 cuc3-105* double mutant had a slightly stronger phenotype than the *cuc3-105* single mutant (Figure 3). The *da1-1 cuc3-105* double mutant also lacked AMs in a few cauline leaf axils and had branches fused to main stems (Figure 3). In addition, overexpression of *DA1* obviously repressed the AM initiation defect of *cuc2-3* and *cuc3-105* (Supplemental Figures 5B to 5D). These genetic analyses suggest that *DA1* functions, at least in part, with *CUC2* and *CUC3* in a common pathway to regulate the initiation of AMs during vegetative growth stage.

CUC2 and CUC3 Directly Bind to the Promoter of *DA1* and Activate Its Expression

DA1 functions genetically with *CUC2* and *CUC3* to control the AM initiation, and CUC2 and CUC3 are two NAC transcription factors. We therefore asked whether CUC2 and CUC3 could regulate the expression of *DA1*. We generated the chemically inducible *CUC2* (*pER8*:*CUC2*) and *CUC3* (*pER8*:*CUC3*) transgenic plants. The expression levels of *DA1* were examined after treating *pER8*:*CUC2* and *pER8*:*CUC3* transgenic plants with β-estradiol (Figure 4A). The expression of *DA1* was significantly elevated after β-estradiol induction. In addition, the expression of *DA1* in *cuc2-3*, *cuc3-105*, and *cuc2-3 cuc3-105* mutants was decreased compared with that in the wild type (Figure 4B). The expression of *DAR1* in *cuc2-3*, *cuc3-105*, and *cuc2-3 cuc3-105* mutants was also decreased compared with that in the wild type (Supplemental Figures 5A). These results indicate that CUC2 and CUC3 regulate the expression of *DA1*.

To determine whether CUC2 and CUC3 can directly associate with the *DA1* promoter, a chromatin immunoprecipitation (ChIP) assay using *35S*:*myc-CUC2*, *35S*:*myc-CUC3*, and *35S*:*myc* transgenic plants was performed. The core sequence CGT[GA] is the DNA binding site of NAC domain transcription factors (Olsen et al., 2005). We identified five candidate binding sequences (A to E) of NAC transcription factors in the 2-kb region of the *DA1* promoter (Figure 4C). A ChIP assay showed that the fragments (PF2, PF3, and PF4) containing the CGT[GA] motif were enriched in the chromatin-immunoprecipitated DNA generated with an anti-myc antibody (Figure 4D). However, the fragment PF5 was not enriched in the chromatin-immunoprecipitated DNA. We also did not detect significant enrichment of the fragments PF1 and PF6, which did not contain the CGT[GA] sequence. Thus, CUC2 and CUC3 associate with the promoter region of *DA1* in vivo.

To investigate whether CUC2 and CUC3 could directly bind to *DA1* promoter, we expressed CUC2 and CUC3 as MBP fusion proteins MBP-CUC2 and MBP-CUC3 and performed DNA electrophoretic mobility shift assays (EMSAs). MBP-CUC2 and MBP-CUC3 could bind to four biotin-labeled probes (A to D) containing the CGT[GA] sequence (Figures 4E and 4F; Supplemental Figures 6A and 6B). However, the DNA–protein association was decreased in a dosage-dependent manner when adding the corresponding unlabeled probes. On the contrary, MBP-CUC2 and MBP-CUC3 failed to bind versions of the probes with mutations (A-m to D-m) in the predicted binding sequence (Figures 4E and 4F; Supplemental Figures 6A and 6B). These results demonstrate that CUC2 and CUC3 directly bind to the promoter of *DA1* and promote the expression of *DA1*.

UBP15 Acts Downstream of DA1 to Control the AM Initiation

To identify downstream components of DA1 in the control of the AM formation, a genetic screen was conducted to isolate the suppressors of *da1-1* in the formation of branches (*sdb*). One of the suppressors, *sdb1-1*, repressed the reduced axillary-branch phenotype of *da1-1* (Figure 5A). The *sdb1-1 da1-1* plants produced more axillary branches than the *da1-1* single mutant (Figure 5A). The axillary bud formation was further examined in axils of *sdb1-1 da1-1* cauline and rosette leaves. As shown in Figure 5B, the pattern of axillary bud formation in the *sdb1-1 da1-1* plants was similar to that in wild-type plants, indicating that the

Figure 3. (continued).

presence of an axillary bud, yellow indicates the absence of an axillary bud in any particular leaf axil, and brown indicates branches fused to the main stem. Plants were grown for 28 d in short photoperiods and subsequently shifted to long days ($n \geq 19$).

(B) Frequency of the lack of axillary shoots in the Col-0, *da1-1*, *cuc2-3*, *da1-1 cuc2-3*, *cuc3-105*, *da1-1 cuc3-105*, *las-101*, *da1-1 las-101*, *rax1-3*, and *da1-1 rax1-3* plants ($n \geq 19$). Values are given as mean ± SD. **$P < 0.01$, compared with *da1-1* plants (Student's *t* test; Supplemental Data Set). ns, no significance.

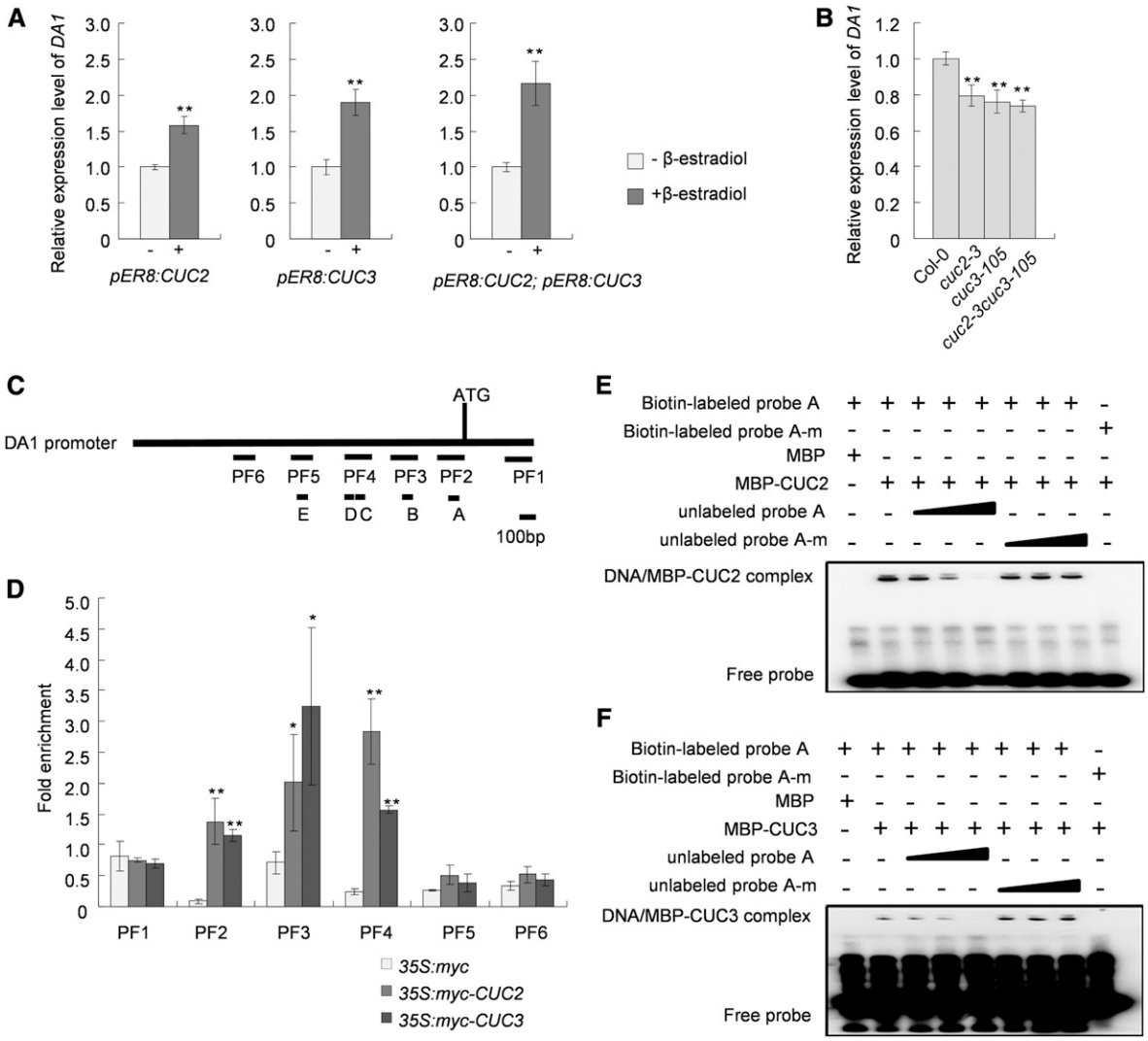

Figure 4. CUC2 and CUC3 Bind to the Promoter of *DA1* and Promote Its Expression.

(A) RT-qPCR analysis of *DA1* expression levels in *pER8*:*CUC2*, *pER8*:*CUC3*, and *pER8*:*CUC2*;*pER8*:*CUC3* seedlings before (–) and after β-estradiol (+) treatment. *ACTIN2* mRNA was used as an internal control. Means were calculated from four biological samples. Values are given as mean ± SD relative to the values before β-estradiol treatment, set at 1. **P < 0.01 (Student's *t* test; Supplemental Data Set).

(B) RT-qPCR analysis of *DA1* expression level in Col-0, *cuc2-3*, *cuc3-105*, and *cuc2-3 cuc3-105* rosette leaf axils. Plants were grown for 28 d in short photoperiods. All rosette leaves were removed, and the base region of petioles and the nonelongated stems were used to isolate total mRNA. *ACTIN2* mRNA was used as an internal control. Means were calculated from four biological samples. Values are given as mean ± SD relative to Col-0 values, set at 1. *P < 0.05, **P < 0.01 compared with Col-0 plants (Student's *t* test; Supplemental Data Set).

(C) A 2.5-kb promoter region of *DA1* upstream of its ATG codon contains five predicted binding sequences named A to E. A, B, C, D, and E and A-m, B-m, C-m, D-m, and E-m indicate the wild-type probes and the mutated probe used in the EMSA, respectively (detailed sequences are listed in the Supplemental Table). PFs represent PCR fragments used for ChIP-qPCR analysis. As the sequence C is very close to sequence D, these two sequences were contained in one fragment PF4. PF2, PF3, and PF5 contain the predicted binding sequence A, B, and E, respectively.

(D) ChIP-qPCR analysis shows that CUC2 and CUC3 bind to the promoter fragments of *DA1*. Chromatin from *35S*:*myc*, *35S*:*myc-CUC2*, and *35S*:*myc-CUC3* transgenic plants were immunoprecipitated by anti-myc, and the enrichment of the fragments was determined by qPCR. Means were calculated from three biological samples. Values are given as mean ± SD. *P < 0.05, **P < 0.01 compared with *35S*:*myc* transgenic plants (Student's *t* test; Supplemental Data Set).

(E) EMSA experiments showed that CUC2 directly binds to the promoter of *DA1*. The biotin-labeled probe A and MBP-CUC2 formed a DNA–protein complex, but the mutated probe A-m and MBP-CUC2 did not. The retarded DNA–protein complex was reduced by the competition using the unlabeled probe A, but not reduced by the competition using the unlabeled mutated probe A-m.

(F) EMSA experiments showed that CUC3 directly binds to the promoter of *DA1*. The biotin-labeled probe A and MBP-CUC3 formed a DNA–protein complex, but the mutated probe A-m and MBP-CUC3 did not. The retarded DNA–protein complex was reduced by the competition using the unlabeled probe A, but not reduced by the competition using the unlabeled mutated probe A-m.

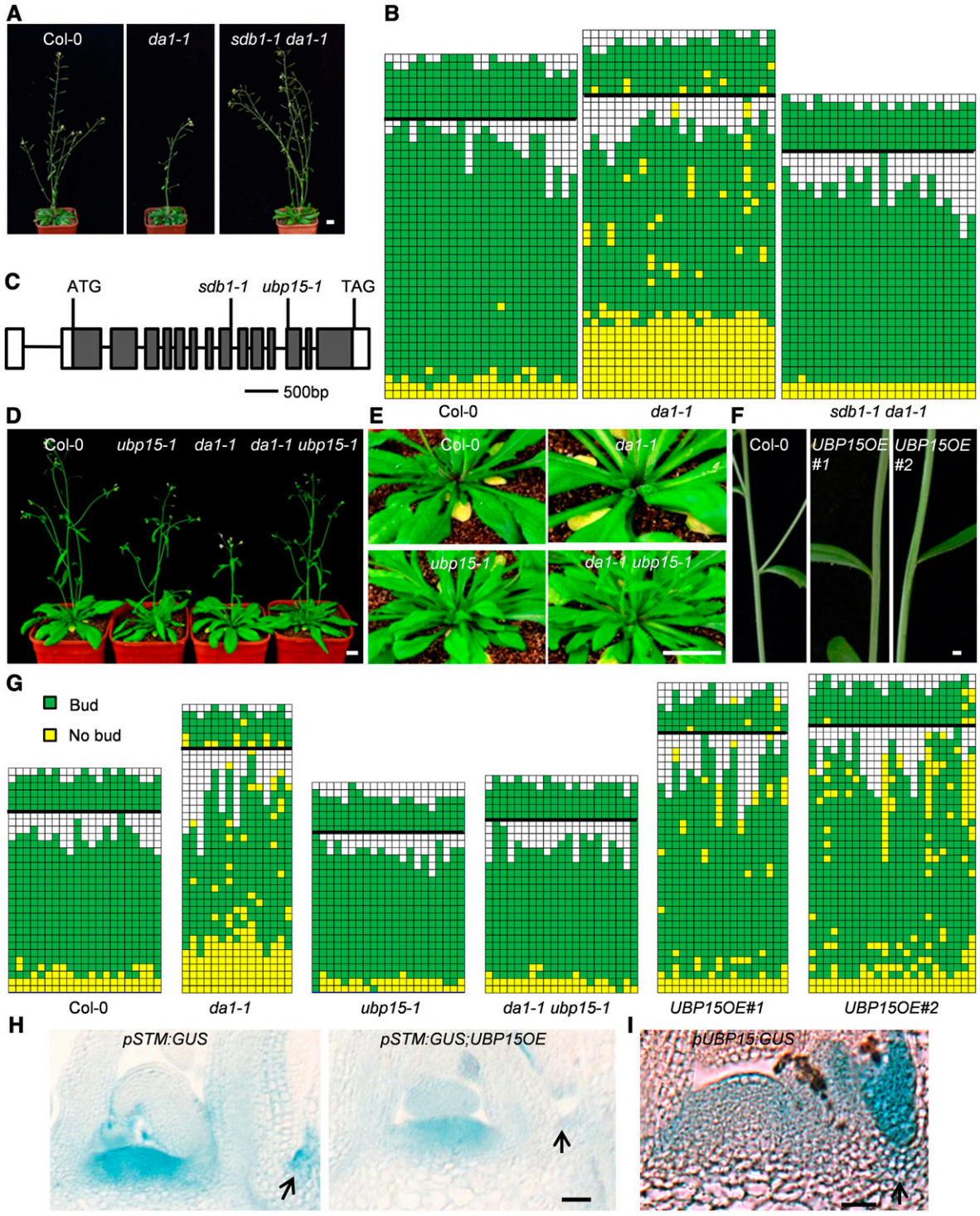

Figure 5. UBP15 Acts Downstream of DA1 to Repress the Initiation of Axillary Meristems.

(A) Plants of Col-0, *da1-1*, and *sdb1-1 da1-1*. Plants were cultivated in short-day conditions for 28 d and then transferred to long-day conditions.
(B) Schematic representation of axillary branch or bud formation in individual leaf axils of Col-0, *da1-1*, and *sdb1-1 da1-1* plants. Green and yellow boxes show the presence or absence of an axillary bud in leaf axils along the main shoot, respectively. Plants were grown for 28 d in short photoperiods and subsequently shifted to long days ($n \geq 24$).
(C) *UBP15* gene structure. The start codon (ATG) and the stop codon (TAG) are indicated. Closed boxes indicate the coding sequence, open boxes indicate the 5′ and 3′ untranslated regions, and lines between boxes indicate introns. The mutation site of *sdb1-1* is shown.

sdb1-1 mutation suppresses the defect of *da1-1* in the AM initiation.

We mapped the *sdb1-1* mutation and observed that the primary mapping region contained *UBIQUITIN-SPECIFIC PROTEASE15* (*UBP15*)/*SUPPRESSOR2 OF DA1* (*SOD2*; Figure 5C; Supplemental Figure 7A). We previously showed that the organ growth phenotype of *da1-1* can be suppressed by mutations in *UBP15* (Du et al., 2014). DA1 mediates the degradation of UBP15 by physically interacting with UBP15 and cleaving UBP15 (Dong et al., 2017). These results imply that *SDB1* could be the *UBP15* gene. Indeed, sequence analyses revealed that *sdb1-1* contained a Gly-to-Ala substitution in the 3′ intron–exon boundary of exon 9 in *UBP15*, resulting in altered splicing of *UBP15* mRNA (Figure 5C; Supplemental Figures 7B to 7D).

We then asked whether the T-DNA insertion mutant *ubp15-1* could influence the formation of axillary buds. As shown in Figures 5D and 5G, the number of axillary buds in *ubp15-1* was only slightly more than that in Col-0, indicating that the *ubp15-1* single mutant very slightly affects the AM initiation. We further investigated the axillary buds of plants overexpressing *UBP15* (*UBP15OE*; Du et al., 2014). As shown in Figure 5G, overexpression of *UBP15* caused the reduced number of axillary buds in both rosette and cauline leaf axils, as observed in *da1-1*, indicating that UBP15 represses the initiation of AMs. *STM* expression was not clearly detected in the leaf axils of *UBP15OE* that failed to produce axillary buds (Figure 5H), further supporting the role of UBP15 in the initiation of AMs. Consistent with the role of UBP15 in the formation of AMs, *UBP15* expression was detected in the shoot meristem, young leaves, and the region between the shoot meristem and leaf primordia (Figure 5I; Du et al., 2014). We further investigated whether *ubp15-1* could suppress the AM initiation phenotype of *da1-1.* As expected, *ubp15-1* completely suppressed the axillary meristem–absence phenotype of *da1-1* (Figures 5D and 5G), indicating that *ubp15-1* was epistatic to *da1-1* with respect to the AM initiation. These results indicate that UBP15 acts downstream of DA1 to control the AM initiation.

UBP15 Acts Genetically with CUC2/CUC3 and LAS to Control the Initiation of AMs

Considering that CUC2 and CUC3 associate with the promoter of *DA1* and promote its expression (Figure 4) and DA1 acts upstream of UBP15 to influence the formation of AMs (Figure 5), we presumed that CUC2 and CUC3 could act in a common pathway with UBP15 to regulate the formation of AMs. To test this, we crossed *ubp15-1* with *cuc2-3* and *cuc3-105* and identified *ubp15-1 cuc2-3* and *ubp15-1 cuc3-105* double mutants, respectively. As shown in Figure 6, *ubp15-1* repressed the AM initiation defect of *cuc2-3* and *cuc3-105*, respectively. The *ubp15-1 cuc2-3* and *ubp15-1 cuc3-105* double mutants produced normal axillary buds like those observed in the wild type. In addition, *cuc3-105* plants showed branches that were fused to the main stems during reproductive development, whereas the *ubp15-1 cuc3-105* double mutants did not show the phenotype of branches fused to main stems during reproductive development (Figure 6). These genetic results imply that UBP15 may function in the same pathway with CUC2 and CUC3 to regulate the initiation of AMs.

DA1 acts synergistically with LAS and RAX1 to promote the initiation of AMs, suggesting that DA1 may act redundantly with LAS and RAX1 to control AM formation. We then asked whether UBP15 could genetically interact with LAS and RAX1 to affect AM initiation. To test this, we crossed *ubp15-1* with *las-101* and *rax1-3* and isolated *las-101 ubp15-1* and *rax1-3 ubp15-1* double mutants, respectively. The *ubp15-1* mutation repressed the AM initiation defect of *las-101* during vegetative development (Figure 6). By contrast, the *ubp15-1* mutation did not obviously repress the AM initiation defect of *rax1-3*. The *las-101* plants showed branches that were fused to main stems during reproductive development. Interestingly, *las-101 ubp15-1* double mutants did not exhibit the phenotype of branches fused to main stems during reproductive development (Figure 6), indicating that *ubp15-1* suppresses the concaulescence phenotype of *las-101*. These findings suggest that UBP15 genetically interacts, at least in part, with LAS to influence the boundary formation.

DISCUSSION

Lateral branches of plants arise from AMs in the region between the SAMs and leaf primordia and are important for plant architecture. The initiation of AMs is a crucial step for generating axillary branches. Several genes have been identified to affect the AM initiation in Arabidopsis (Greb et al., 2003; Hibara et al., 2006; Keller et al., 2006; Müller et al., 2006; Raman et al., 2008), but the mechanisms of AM initiation are still largely unknown. Here, we uncover a genetic and molecular framework in which a CUC2/CUC3-DA1-UBP15 regulatory module controls the formation of AMs, thereby determining plant architecture.

Figure 5. (continued).

(D) Fifty-five-day-old plants of Col-0, *da1-1*, *ubp15-1*, and *da1-1 ubp15-1*. Plants were cultivated in short-day conditions for 28 d and then transferred to long-day conditions.

(E) Close-up views of rosette leaf branches in rosette leaf axils of Col-0, *da1-1*, *ubp15-1*, and *da1-1 ubp15-1*.

(F) Close-up views of cauline leaf branches in cauline leaf axils of Col-0, *UBP15OE#1*, and *UBP15OE#2*.

(G) Schematic representation of axillary branch or bud formation in individual leaf axils of Col-0, *da1-1*, *ubp15-1*, *da1-1 ubp15-1*, *UBP15OE#1*, and *UBP15OE#2* ($n \geq 15$).

(H) *pSTM*:*GUS* expression in longitudinal sections of Col-0 and *UBP15OE*. GUS signal is reduced in leaf axils of *UBP15OE* plants. Plants were grown for 28 d in short photoperiods.

(I) *UBP15* expression activity was monitored using *pUBP15*:*GUS* transgenic plants. GUS activity was detected in longitudinal sections through the vegetative shoot apex. Plants were grown for 28 d in short-day conditions.

Bar in **(A)**, **(D)**, and **(E)** = 1 cm; bar in **(F)** = 1 mm; bar in **(H)** and **(I)** = 20 μm.

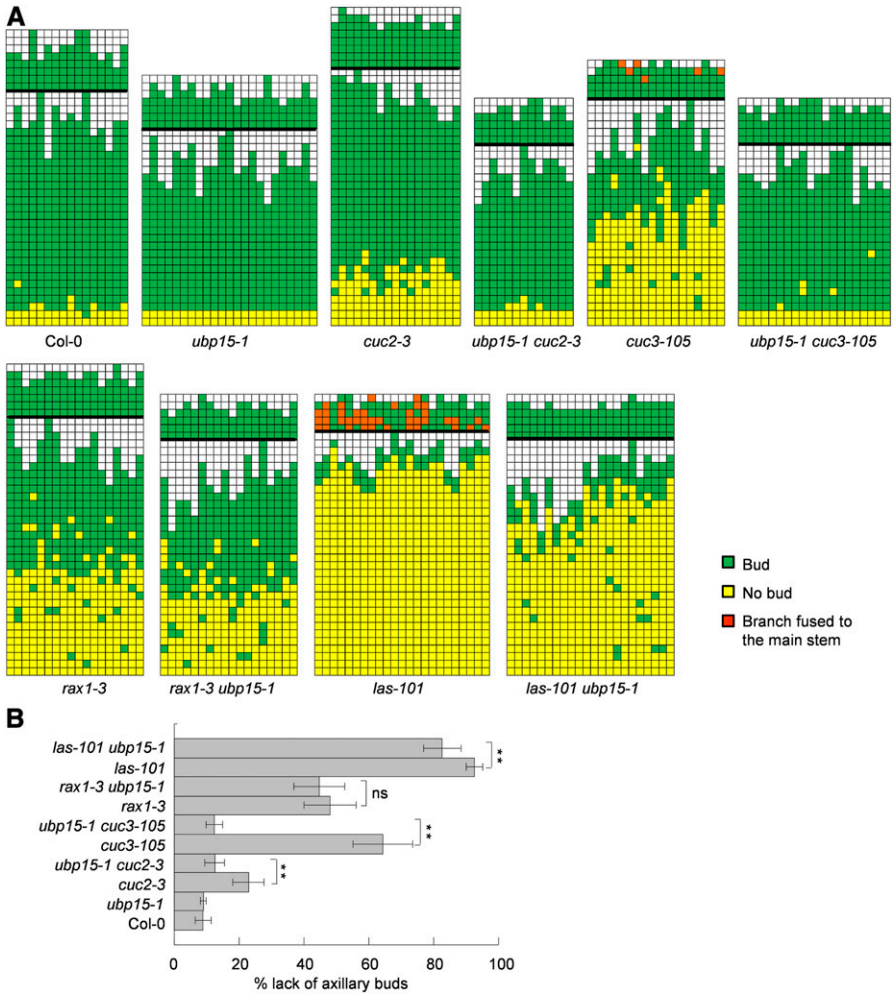

Figure 6. *UBP15* Acts in a Common Pathway with *CUC2* and *CUC3.*

(A) Schematic representation of axillary branch or bud formation in individual leaf axils of Col-0, *ubp15-1*, *cuc2-3*, *ubp15-1 cuc2-3*, *cuc3-105*, *ubp15-1 cuc3-105*, *rax1-3*, *rax1-3 ubp15-1*, *las-101*, and *las-101 ubp15-1* plants ($n \geq 13$). The thick black horizontal lines represent the border between the youngest rosette leaf and the oldest cauline leaf, with positions of progressively younger cauline leaves above the line, and positions of progressively older rosette leaves below the line. Each column represents a single plant, and each square within a column represents an individual leaf axil shown from youngest (top) to oldest. Green indicates the presence of an axillary bud, and yellow indicates the absence of an axillary bud in any particular leaf axil. Plants were grown for 28 d in short photoperiods and subsequently shifted to long days ($n \geq 13$).

(B) Frequency of the lack of axillary shoots in the Col-0, *ubp15-1*, *cuc2-3*, *ubp15-1 cuc2-3*, *cuc3-105*, *ubp15-1 cuc3-105*, *rax1-3*, *rax1-3 ubp15-1*, *las-101*, and *las-101 ubp15-1* plants ($n \geq 13$). Values are given as mean ± SD. **P < 0.01 compared with *da1-1* plants (Student's *t* test). ns, no significance.

The ubiquitin-dependent peptidase DA1 has been described to negatively control organ growth in Arabidopsis (Li et al., 2008; Dong et al., 2017). Here, we observed that the *da1-1* mutation disrupted AM initiation in the axils of rosette and cauline leaves, resulting in fewer axillary branches. Supporting the function of DA1 in the initiation of AMs, expression of the meristem marker gene *STM* in *da1-1* was undetectable in the axils of leaves that did not produce axillary buds (Figure 2C). *DA1* is expressed in the SAM and the region between SAM and leaf primordium (Figure 2B). These results demonstrate that DA1 positively regulates AM initiation. DA1 has been reported to control organ growth by influencing cell proliferation (Li et al., 2008). How DA1 regulates both cell proliferation and the AM establishment is an interesting question. Considering that DA1 limits cell proliferation and promotes cell differentiation, it is possible that the balance between cell proliferation and cell differentiation might be crucial for the initiation of AMs in the leaf axils. It will be a difficult but worthwhile challenge to investigate this possibility in the future.

NAC transcription factors CUC2 and CUC3 are positive regulators of the AM initiation (Hibara et al., 2006). The genetic analyses suggest that DA1 functions, at least in part, in a common pathway with CUC2 and CUC3 to regulate the AM initiation (Figure 3). Consistent with this, we showed that CUC2 and CUC3 directly associate with the promoter region of *DA1* and activate its expression (Figure 4). We further investigated the genetic interaction of DA1 with LAS and RAX1 and observed that DA1 functions

synergistically with LAS and RAX1 in the regulation of AM initiation (Figure 3; Supplemental Figure 4), suggesting that DA1 may function redundantly with LAS and RAX1 to regulate the formation of AMs. To identify downstream components of DA1 in the AM formation, we isolated suppressors of *da1-1* in the formation of branches and concluded that one of them is a novel allele of the ubiquitin-specific protease *UBP15*.

We have previously demonstrated that DA1 interacts with and cleaves UBP15, resulting in its degradation (Du et al., 2014; Dong et al., 2017). In accordance with this biochemical data, *ubp15-1* completely suppressed the defect of the AM initiation of *da1-1*, indicating that UBP15 acts downstream of DA1 to control the initiation of AMs (Figure 5). *upb15-1* also suppressed the AM initiation defect of *cuc2-3* and *cuc3-105*, respectively (Figure 6). These results suggest that CUC2/CUC3, DA1, and UBP15 function in a common pathway to control the initiation of AMs. By contrast, *upb15-1* only slightly suppressed the AM initiation defect of *las-101*. Interestingly, *ubp15-1* completely suppressed the phenotype of branches fused to main stems in *las-101* (Figure 6). These findings suggest that UBP15 might have partially overlapping function with LAS in the regulation of the boundary formation. It is also possible that UBP15 may slightly mediate the effect of LAS on the initiation of AMs.

Based on our data, we propose a working model that CUC2 and CUC3 directly associate with the promoter of *DA1* and activate its expression and that DA1 then interacts with UBP15 and promotes the degradation of UBP15 to regulate the initiation of AMs (Figure 7). Considering that the *cuc2 cuc3* double mutant has stronger defects in the initiation of AMs than *da1-1* (Hibara et al., 2006), it is plausible that CUC2 and CUC3 may have other downstream targets. Supporting this notion, LAS has been proposed to act downstream of *CUC2* (Hibara et al., 2006; Raman et al., 2008; Tian et al., 2014). *DA1* functions redundantly with *LAS* to control the initiation of AMs. Taken together, our findings point to a genetic and molecular framework in which CUC2/CUC3-DA1-UBP15 regulatory module–mediated control of the AM initiation influences plant lateral branch number.

The number of lateral branches is an important component of plant architecture, which has been recognized as a target for breeding. It is believed that crops with ideal plant architecture will be highly efficient in their use of light, nutrients, and space and should produce high yields (Wang and Li, 2008). Although the detailed standards of ideal plant architecture are different among different kinds of crops, all models contain the requirement for an appropriate number of lateral branches. In this study, we have identified CUC2/CUC3-DA1-UBP15 as a regulatory module for lateral branches. Therefore, it will be worthwhile to investigate whether homologs of CUC2, CUC3, DA1, and UBP15 could be used to improve plant architecture in key crops.

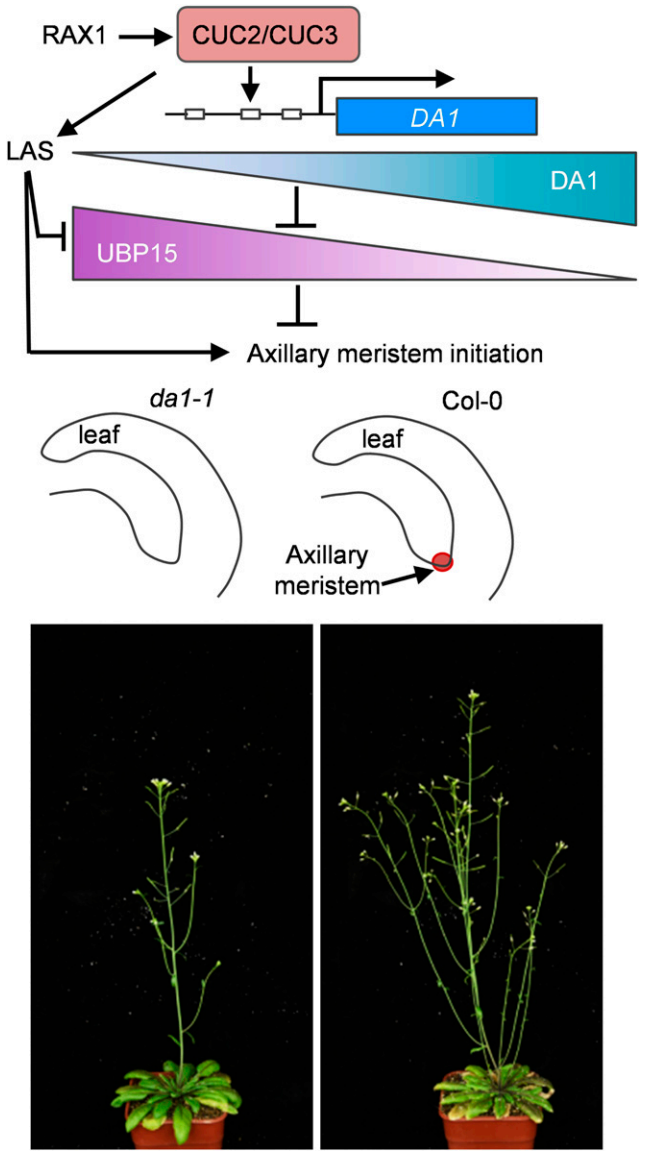

Figure 7. CUC2/CUC3-DA1-UBP15 Regulatory Module-Mediated Control of Axillary Meristem Initiation.

CUC2 and CUC3 directly bind to the promoter region of *DA1* and activate its expression. DA1 is a positive regulator of the initiation of AMs. DA1 promotes the degradation of UBP15 that represses the initiation of AMs. DA1 functions redundantly with LAS to promote the initiation of AMs. UBP15 also partially mediates the effect of LAS on the initiation of AMs.

METHODS

Plant Material and Growth Conditions

The *las-101* (SALK_000896), *cuc3-105* (ABI_302G09), *cuc2-3* (SAIL_605_C09), *rax1-3* (SALK_071748), and *ubp15-1* (SALK_018601) mutants were obtained from Nottingham Arabidopsis Stock Centre and Arabidopsis Biological Resources Center (Hibara et al., 2006). The *da1-1*, *da1-ko1 dar1-1*, *DA1COM*, *35S:DA1$^{R/K}$*, *35S:DA1*, *pDA1:GUS*, *pUBP15:GUS*, *pSTM:GUS*, *UBP15OE*, and *da1-1 ubp15-1* mutants were described previously (Li et al., 2008; Du et al., 2014). The *da1-1 las-101*, *da1-1 rax1-3*, *da1-1 cuc2-3*, and *da1-1 cuc3-105* double mutants were generated by crossing *da1-1* with *las-101*, *rax1-3*, *cuc2-3*, and *cuc3-105*, respectively. The *ubp15-1 cuc2-3*, *ubp15-1 cuc3-105*, *rax1-3 ubp15-1*, and *las-101 ubp15-1* double mutants were generated by crossing *ubp15-1* with *cuc2-3*, *cuc3-105*, *rax1-3*, and *las-101*, respectively. The *sdb1-1 da1-1* double mutant was isolated from an M2 population of *da1-1* treated with ethyl methanesulfonate. T-DNA insertion mutants were identified by PCR with primers listed in the

Supplemental Table. Seeds were sterilized using 10% (v/v) household bleach for 10 min, washed with sterile water at least three times, stratified for 3 d in dark at 4°C before plating on half-strength Murashige and Skoog (MS) medium with 1% Glu, and germinated at 22°C. For short-day conditions, seedlings were grown at 22°C with 70% RH, and an 8-h-light/16-h-dark cycle in a controlled environmental chamber. For long-day conditions, seedlings were grown at 22°C and a 16-h-light/8-h-dark cycle in a controlled environmental chamber or in a greenhouse. The light intensity was ~120 μmol $m^{-2} \cdot s^{-1}$ provided by white fluorescent tubes.

Constructs and Transformation

To generate *35S:myc-CUC2* and *35S:myc-CUC3*, the coding sequences of *CUC2*/*CUC3* were amplified with primers listed in the Supplemental Table (myc-CUC2-F/R and myc-CUC3-F/R). The products were then cloned into the *Bam*HI/*Sac*I sites of *pCAMBIA1300-221-myc*. *35S:myc-CUC2* and *35S:myc-CUC3* plasmids were transformed into Arabidopsis *cuc2-3* and *cuc3-105* mutants plants using *Agrobacterium tumefaciens* GV3101. To generate *pER8:CUC2* and *pER8:CUC3*, the coding sequences of *CUC2*/*CUC3* were amplified with primers listed in the Supplemental Table (pER8-CUC2-F/R and pER8-CUC3-F/R). The products were then cloned into the *Xho*I/*Pac*I sites of *pER8* vector. The plasmids were transformed into Arabidopsis (*Arabidopsis thaliana*) Col-0 plants using *A. tumefaciens* GV3101. Transgenic plants were grown on half-strength MS medium with 1% Glu containing hygromycin (30 μg/mL).

RNA Isolation and RT-qPCR Analysis

RNAprep pure plant kit was used to extract the total RNA (Tiangen). Total mRNA was reverse transcribed into cDNA using SuperScript III reverse transcriptase (Invitrogen). The Bio-Rad CFX96 machine was used for RT-qPCR analysis using RealStar Green Fast Mixture (A301-05, GenStar). The relative expression level of gene was evaluated using the cycle threshold method. *ACTIN2* was used as the reference gene. Seedlings (28 d old) were grown under short-day photoperiods. After all rosette leaves of seedlings were removed, the base region of petioles and the nonelongated stems were used for RNA extraction. Gene-specific primers (Supplemental Table) were used for RT-PCR and RT-qPCR. Error bars are derived from four independent biological experiments, each run in triplicate.

Analysis of Axillary Shoot and Bud Formation

For the analysis of shoot formation, plants were grown under short-day photoperiods for 28 d before being transferred to the long-day conditions. The formation of bud or branch in leaf axils was analyzed at 14 d after the onset of flowering. The shoot or bud formation was investigated by stereomicroscope. For each experiment, at least 13 plants were investigated. Each experiment was repeated at least three times.

Scanning Electron Microscopy

Scanning electron microscopy was performed using a Hitachi S-3000N variable pressure scanning electron microscope. Samples were fixed in formalin–acetic acid–alcohol solution by vacuum treatment for 30 min. Fixed samples were dehydrated with a gradual ethanol series, dried by critical-point drying, and subsequently coated with a gold layer.

GUS Staining

For the GUS activity analysis of *pDA1:GUS* and *pUBP15:GUS* transgenic plants, seedlings were grown for 28 d in short-day conditions. The method for GUS staining was used as previously described by Sessions et al. (1999).

ChIP Assay

ChIP assay was performed according to protocols previously described by Gendrel et al. (2005), with minor modifications. The transgenic seeds of *35S:myc-CUC2*, *35S:myc-CUC3*, and *35S:myc* were grown on GM medium for 10 d. The plants were harvested and cross-linked with 1% (v/v) formaldehyde. The chromatin complexes were isolated and sonicated. The chromatin was immunoprecipitated by protein A+G magnetic beads (16-663, Merck Millipore) and anti-myc (ab32, lot no. GR310953-4, Abcam). The precipitated DNA was purified and dissolved in water. Primers used for the ChIP assay are listed in the Supplemental Table (PF1-F, PF1-R, PF2-F, PF2-R, PF3-F, PF3-R, PF4-F, PF4-R, PF5-F, PF5-R, PF6-F, PF6-R, ACTIN7 -F, and ACTIN7 -R).

EMSA

The coding sequences of *CUC2* and *CUC3* were amplified using primers (MBP-CUC2-F/R and MBP-CUC3-F/R) and then cloned into the *Eco*RI/*Pst*I sites of *pMAL-c2* to generate the *MBP-CUC2*/*CUC3* constructs. The primers are listed in the Supplemental Table. Bacterial lysates expressing MBP-CUC2/CUC3 were extracted from *Escherichia coli* BL21 (DE3). Bacterial cells were lysed using the PBS buffer (2.7 mM KCl, 137 mM NaCl, 1.4 mM KH_2PO_4, and 4.3 mM Na_2HPO_4, pH 7.4) and then sonicated. The MBP-CUC2 and MBP-CUC3 proteins were purified using amylose resin (E8021L, New England Biolabs). EMSAs were performed according to the method previously described by Zhang et al. (2015). The biotin-labeled probes were synthesized. MBP-fusion proteins were incubated with biotin-labeled probes for 30 min at 22°C. The competition experiments were performed by adding 10- to 1000-fold unlabeled DNA.

Accession Numbers

The accession numbers are as follows: *CUC2* (At5g53950), *CUC3* (At1g76420), *DA1* (At1g19270), *DAR1* (At4g36860), *SOD2*/*UBP15* (At1g17110), *LAS* (At1g55580), and *RAX1* (At5g23000).

Supplemental Data

Supplemental Figure 1. *da1-1* influences the branch phenotype (Supports Figure 1).

Supplemental Figure 2. *35S:DA1$^{R/K}$* influences the branch phenotype (Supports Figure 1).

Supplemental Figure 3. *35S:DA1* slightly influences the branch phenotype (Supports Figure 1).

Supplemental Figure 4. Genetic interactions of *DA1* with *LAS* and *RAX1* (Supports Figure 3).

Supplemental Figure 5. Genetic interactions of *DA1* with *CUC2* and *CUC3* (Supports Figure 3).

Supplemental Figure 6. CUC2 and CUC3 directly bind to the promoter of *DA1* (Supports Figure 4).

Supplemental Figure 7. Identification of *UBP15* (Supports Figure 5).

Supplemental Table. List of primers used in this study.

Supplemental Data Set. Statistical analysis.

ACKNOWLEDGMENTS

We thank Jiayang Li for his critical reading of this article. We thank Masao Tasaka, Nottingham Arabidopsis Stock Centre, and Arabidopsis Biological Resources Center for *las-101*, *cuc2-3*, *cuc3-105*, and *rax1-3* seeds and

Nam-Hai Chua for the *pER8* vector. This work was supported by the National Natural Science Foundation of China (grants 3181101602, 31961133001, and 31425004) and the strategic priority research program of the Chinese Academy of Sciences (grant XDB27010102).

AUTHOR CONTRIBUTIONS

Yu.L., T.X., and F.G. performed experiments. Yu.L., T.X., and Y.L. analyzed data. Yu.L. and Y.L. wrote the article.

Received January 7, 2020; revised February 18, 2020; accepted March 26, 2020; published April 2, 2020.

REFERENCES

Aida, M., Ishida, T., Fukaki, H., Fujisawa, H., and Tasaka, M. (1997). Genes involved in organ separation in Arabidopsis: An analysis of the cup-shaped cotyledon mutant. Plant Cell **9:** 841–857.

Barbier, F.F., Dun, E.A., Kerr, S.C., Chabikwa, T.G., and Beveridge, C.A. (2019). An update on the signals controlling shoot branching. Trends Plant Sci. **24:** 220–236.

Brewer, P.B., Dun, E.A., Gui, R., Mason, M.G., and Beveridge, C.A. (2015). Strigolactone inhibition of branching independent of polar auxin transport. Plant Physiol. **168:** 1820–1829.

Brewer, P.B., Koltai, H., and Beveridge, C.A. (2013). Diverse roles of strigolactones in plant development. Mol. Plant **6:** 18–28.

Domagalska, M.A., and Leyser, O. (2011). Signal integration in the control of shoot branching. Nat. Rev. Mol. Cell Biol. **12:** 211–221.

Dong, H., et al. (2017). Ubiquitylation activates a peptidase that promotes cleavage and destabilization of its activating E3 ligases and diverse growth regulatory proteins to limit cell proliferation in *Arabidopsis*. Genes Dev. **31:** 197–208.

Du, L., Li, N., Chen, L., Xu, Y., Li, Y., Zhang, Y., Li, C., and Li, Y. (2014). The ubiquitin receptor DA1 regulates seed and organ size by modulating the stability of the ubiquitin-specific protease UBP15/SOD2 in Arabidopsis. Plant Cell **26:** 665–677.

Flematti, G.R., Scaffidi, A., Waters, M.T., and Smith, S.M. (2016). Stereospecificity in strigolactone biosynthesis and perception. Planta **243:** 1361–1373.

Gendrel, A.V., Lippman, Z., Martienssen, R., and Colot, V. (2005). Profiling histone modification patterns in plants using genomic tiling microarrays. Nat. Methods **2:** 213–218.

Grbic, V., and Bleecker, A.B. (2000). Axillary meristem development in *Arabidopsis thaliana*. Plant J. **21:** 215–223.

Greb, T., Clarenz, O., Schafer, E., Muller, D., Herrero, R., Schmitz, G., and Theres, K. (2003). Molecular analysis of the LATERAL SUPPRESSOR gene in Arabidopsis reveals a conserved control mechanism for axillary meristem formation. Genes Dev. **17:** 1175–1187.

Hibara, K., Karim, M.R., Takada, S., Taoka, K., Furutani, M., Aida, M., and Tasaka, M. (2006). Arabidopsis CUP-SHAPED COTYLEDON3 regulates postembryonic shoot meristem and organ boundary formation. Plant Cell **18:** 2946–2957.

Janssen, B.J., Drummond, R.S., and Snowden, K.C. (2014). Regulation of axillary shoot development. Curr. Opin. Plant Biol. **17:** 28–35.

Keller, T., Abbott, J., Moritz, T., and Doerner, P. (2006). Arabidopsis REGULATOR OF AXILLARY MERISTEMS1 controls a leaf axil stem cell niche and modulates vegetative development. Plant Cell **18:** 598–611.

Kirch, T., Simon, R., Grünewald, M., and Werr, W. (2003). The DORNROSCHEN/ENHANCER OF SHOOT REGENERATION1 gene of Arabidopsis acts in the control of meristem cell fate and lateral organ development. Plant Cell **15:** 694–705.

Lee, D.K., Geisler, M., and Springer, P.S. (2009). LATERAL ORGAN FUSION1 and LATERAL ORGAN FUSION2 function in lateral organ separation and axillary meristem formation in Arabidopsis. Development **136:** 2423–2432.

Li, Y., Zheng, L., Corke, F., Smith, C., and Bevan, M.W. (2008). Control of final seed and organ size by the DA1 gene family in *Arabidopsis thaliana*. Genes Dev. **22:** 1331–1336.

Long, J., and Barton, M.K. (2000). Initiation of axillary and floral meristems in Arabidopsis. Dev. Biol. **218:** 341–353.

McSteen, P., and Leyser, O. (2005). Shoot branching. Annu. Rev. Plant Biol. **56:** 353–374.

Müller, D., and Leyser, O. (2011). Auxin, cytokinin and the control of shoot branching. Ann. Bot. **107:** 1203–1212.

Müller, D., Schmitz, G., and Theres, K. (2006). Blind homologous R2R3 Myb genes control the pattern of lateral meristem initiation in Arabidopsis. Plant Cell **18:** 586–597.

Müller, D., Waldie, T., Miyawaki, K., To, J.P.C., Melnyk, C.W., Kieber, J.J., Kakimoto, T., and Leyser, O. (2015). Cytokinin is required for escape but not release from auxin mediated apical dominance. Plant J. **82:** 874–886.

Napoli, C.A., Beveridge, C.A., and Snowden, K.C. (1999). Reevaluating concepts of apical dominance and the control of axillary bud outgrowth. Curr. Top. Dev. Biol. **44:** 127–169.

Olsen, A.N., Ernst, H.A., Lo Leggio, L., and Skriver, K. (2005). DNA-binding specificity and molecular functions of NAC transcription factors. Plant Sci. **169:** 785–797.

Otsuga, D., DeGuzman, B., Prigge, M.J., Drews, G.N., and Clark, S.E. (2001). REVOLUTA regulates meristem initiation at lateral positions. Plant J. **25:** 223–236.

Pautler, M., Tanaka, W., Hirano, H.Y., and Jackson, D. (2013). Grass meristems I: Shoot apical meristem maintenance, axillary meristem determinacy and the floral transition. Plant Cell Physiol. **54:** 302–312.

Raman, S., Greb, T., Peaucelle, A., Blein, T., Laufs, P., and Theres, K. (2008). Interplay of miR164, CUP-SHAPED COTYLEDON genes and LATERAL SUPPRESSOR controls axillary meristem formation in *Arabidopsis thaliana*. Plant J. **55:** 65–76.

Schmitz, G., and Theres, K. (2005). Shoot and inflorescence branching. Curr. Opin. Plant Biol. **8:** 506–511.

Schmitz, G., Tillmann, E., Carriero, F., Fiore, C., Cellini, F., and Theres, K. (2002). The tomato Blind gene encodes a MYB transcription factor that controls the formation of lateral meristems. Proc. Natl. Acad. Sci. USA **99:** 1064–1069.

Sessions, A., Weigel, D., and Yanofsky, M.F. (1999). The *Arabidopsis thaliana* MERISTEM LAYER 1 promoter specifies epidermal expression in meristems and young primordia. Plant J. **20:** 259–263.

Smith, S.M., and Li, J. (2014). Signalling and responses to strigolactones and karrikins. Curr. Opin. Plant Biol. **21:** 23–29.

Tantikanjana, T., Yong, J.W., Letham, D.S., Griffith, M., Hussain, M., Ljung, K., Sandberg, G., and Sundaresan, V. (2001). Control of axillary bud initiation and shoot architecture in Arabidopsis through the SUPERSHOOT gene. Genes Dev. **15:** 1577–1588.

Tian, C., et al. (2014). An organ boundary-enriched gene regulatory network uncovers regulatory hierarchies underlying axillary meristem initiation. Mol. Syst. Biol. **10:** 755.

Wang, B., Smith, S.M., and Li, J. (2018). Genetic regulation of shoot architecture. Annu. Rev. Plant Biol. **69:** 437–468.

Wang, Q., Kohlen, W., Rossmann, S., Vernoux, T., and Theres, K. (2014a). Auxin depletion from the leaf axil conditions competence for axillary meristem formation in Arabidopsis and tomato. Plant Cell **26:** 2068–2079.

Wang, Y., and Li, J. (2008). Molecular basis of plant architecture. Annu. Rev. Plant Biol. **59:** 253–279.

Wang, Y., Wang, J., Shi, B., Yu, T., Qi, J., Meyerowitz, E.M., and Jiao, Y. (2014b). The stem cell niche in leaf axils is established by auxin and cytokinin in Arabidopsis. Plant Cell **26:** 2055–2067.

Waters, M.T., Brewer, P.B., Bussell, J.D., Smith, S.M., and Beveridge, C.A. (2012). The Arabidopsis ortholog of rice DWARF27 acts upstream of MAX1 in the control of plant development by strigolactones. Plant Physiol. **159:** 1073–1085.

Xia, T., Li, N., Dumenil, J., Li, J., Kamenski, A., Bevan, M.W., Gao, F., and Li, Y. (2013). The ubiquitin receptor DA1 interacts with the E3 ubiquitin ligase DA2 to regulate seed and organ size in Arabidopsis. Plant Cell **25:** 3347–3359.

Zhang, Y., Du, L., Xu, R., Cui, R., Hao, J., Sun, C., and Li, Y. (2015). Transcription factors SOD7/NGAL2 and DPA4/NGAL3 act redundantly to regulate seed size by directly repressing KLU expression in *Arabidopsis thaliana*. Plant Cell **27:** 620–632.